Dilating behavior of overconsolidated clay

Mahdia Hattab, Pierre-Yves Hicher

DILATING BEHAVIOUR OF OVERCONSOLIDATED CLAY

MAHDIA HATTAB[i] and PIERRE-YVES HICHER[ii]

[i] Associate Professor, Laboratoire de Physique et mécanique des matériaux, ISGMP-UMR CNRS 75045 Ile du Saulcy-57045 Metz Cedex1, France (hattab@lpmm.univ-metz.fr).

[ii] Professor, Laboratoire de Génie Civil de Nantes-Saint Nazaire, Ecole Centrale de Nantes, B.P. 92101, 44321 Nantes Cedex 3, France.

ABSTRACT

The object of this study was to understand and characterize dilatancy in clay in relation to the overconsolidation ratio. This phenomenon was investigated along a large range of loading paths, with strong emphasis placed on constant mean stress paths given that it was possible to measure the volumetric strain created by the sole deviatoric stress. Triaxial tests performed on remolded clay (Kaolinite P300) allowed us to determine three different types of behaviour for specimen submitted to a deviatoric stress: no volume change, dilatancy and contraction. In the (p', q) plane these domains are limited by the maximum strength envelope ζ, which coincides with the perfect plasticity line M for OCRs < 2. The experimental results were then compared to plastic flow theories used in the Cam Clay model and in Rowe's dilatancy theory. Finally, by measuring the plastic strain increment vectors along different stress paths in the (p', q) plane, we demonstrated that the uniqueness hypothesis of the plastic potential is not valid. The results could be explained by using two plastic strain mechanisms: a deviatoric one and an isotropic one.

Key words: dilatancy, overconsolidation ratio, plastic strain mechanisms, triaxial compression tests

INTRODUCTION

Dilatancy was first put forward by Reynolds (1885). He demonstrated that the volume change of a regular packing of rigid spheres under shear depended on the initial arrangement of the spheres and that contraction would occur in a loose packing whereas dilatancy would occur in a dense packing. Consequently the shear strength of the sphere assembly depended not only on the friction between the spheres, as one used to assume, but also on the volume change. Therefore, the Coulomb-Rankine relation had to be extended in order to take into account the dilatancy effects.

In the steps of this pioneer work, many other experimental studies on remolded soils, particularly sands, have improved our understanding of this phenomenon. Drained triaxial test results on sands showed clearly that the initial density is an important parameter, which has a great influence on the dilatancy rate. Dilatancy is more pronounced when the sand is initially in a dense state (Taylor, 1948). In undrained triaxial tests, the dilatant behaviour of dense sand leads to a pore pressure decrease, while a pore pressure increase is obtained in loose samples (Bishop and Henkel, 1962). In the case of clay materials, the results of drained (and undrained) tests showed that the volume change (or pore pressure evolution) during shearing depends mainly on the clay loading history expressed by the overconsolidation ratio. These experimental studies showed that clay behaviour is qualitatively close to sand behaviour. Therefore, the results obtained in sandy materials can highlight different phenomena which can also be found in clayed materials (Biarez and Hicher, 1994).

Analyzing drained triaxial test results at constant lateral stress on sands, Kirkpatrick (1961) demonstrated that the change in behaviour from contractant at low stress ratios to dilatant at high stress ratios was obtained for a given value of $(\sigma_1'/\sigma_3')_c$, independent of the initial consolidation pressure and of the initial density. Rowe (1962) confirmed this result and introduced a relationship between the stress ratio and the dilatancy rate. This particular stress ratio was subsequently generalized to introduce the notions of phase transformation (Ishihara and Okada, 1978) and characteristic state (Luong, 1978), which defined a particular friction angle called φ_c, intrinsic to the material. φ_c or the corresponding slope η_c in the (p', q) plane separates the stress space in two regions: a region of contractant behaviour for stress ratios lower than φ_c and a region of dilatant behaviour for stress ratio higher than φ_c. Stress-Strain behaviour, on the other hand, has been also investigated on different strain paths (Asaka et al., 2003).

Experimental results on clays, on the other hand, are less numerous. Drained and undrained triaxial tests published by Henkel (1956) showed that the volume change for clayed materials depended mainly on the overconsolidation ratio (OCR). Normally consolidated or slightly overconsolidated samples showed a con-

tractant behaviour, while highly overconsolidated samples showed a dilatant behaviour. Similar results were obtained by Zervoyannis (1982) who showed that dilatancy phenomena appeared generally for $2<OCR<2.5$ depending on the clay mineralogy. Shimizu (1982) performed triaxial tests at constant mean effective stress on Fujinanori clay with different overconsolidation ratios. He showed that the (p', q) plane could be divided into several regions of contractant and dilatant behaviours according to the stress level q/p' and the OCR. These first experimental clay studies showed that clay behaviour is similar to sand behaviour. Contractancy or dilatancy in sand are directly connected to the relative density, while in clays these volumetric changes can be more precisely related to the overconsolidation ratio.

TESTING PROCEDURE

In soils, as in other porous media, the application of a stress tensor $\underline{\underline{\sigma'}}$ generates volume changes. $\underline{\underline{\sigma'}}$ can be divided into two parts: the deviatoric part $q \cdot \underline{\underline{D}}$ and the isotropic part $p' \cdot \underline{\underline{I}}$, such as:

$$\underline{\underline{\sigma'}} = q \cdot \underline{\underline{D}} + p' \cdot \underline{\underline{I}} \qquad (1)$$

In the special case of an axisymmetric compression test, the isotropic stress is defined by $p' = \sigma_1' + 2\sigma_3'/3$; and the deviatoric part of the stress tensor by $q = \sigma_1' - \sigma_3'$. σ_1' is the major principal effective stress and σ_3' is the minor principal effective stress. The relation (1) shows that the stress tensor is a combination of the deviatoric tensor and the isotropic tensor. An increase of the isotropic stress always generates a contractive volumetric strain $d\varepsilon_v^{(i)} > 0$; while an increase of the deviatoric part of the stress tensor produces a volumetric strain which can be positive or negative, i.e. $d\varepsilon_v^{(i)} > 0$ for contractant material or $d\varepsilon_v^{(d)} < 0$ for dilatant material. As it will be demonstrated later in the case of clay, the sign of $d\varepsilon_v^{(d)}$ depends highly on the overconsolidation ratio (OCR).

Dilatancy will be defined here as the volume increase characterized by $d\varepsilon_v^{(d)} < 0$, and caused by the increase of the deviatoric part of the stress tensor q. In a classical triaxial test (σ_3' = constant) there is an increase of the mean pressure p' at the same time as of the deviatoric stress q. Thus we obtain a volumetric total strain increment $d\varepsilon_v^{(T)}$ which is the result of the combination between the two effects of the stress tensor, i.e. $d\varepsilon_v^{(i)}$ and $d\varepsilon_v^{(d)}$:

$$d\varepsilon_v^{(T)} = d\varepsilon_v^{(i)} + d\varepsilon_v^{(d)} \qquad (2)$$

In these conditions, characterizing dilatancy can be difficult, because we measure the total volumetric strain $d\varepsilon_v^{(T)}$ experimentally, but we have no access to each part of it.

The approach proposed here is based on the analysis of pure deviatoric stress paths in the triaxial cell. It consists of studying clay samples with several OCR, as shown in Fig. 1. The clay samples are first isotropically consolidated up to a given isotropic stress and then isotropically unloaded in order to obtain a given value of the overconsolidation ratio. The following loading stage consists of applying a deviatoric stress while keeping constant the mean stress. During this second stage, one can have direct access to the volumetric strain increment due to the deviatoric part of the stress tensor:

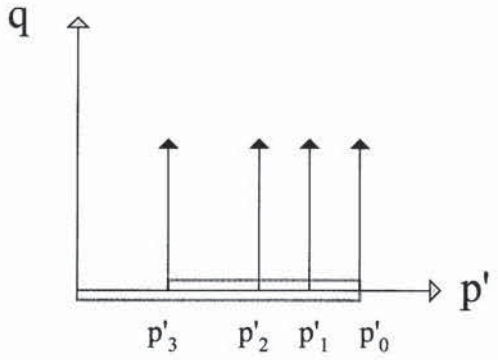

Fig. 1. Constant mean stress paths on overconsolidated clay samples

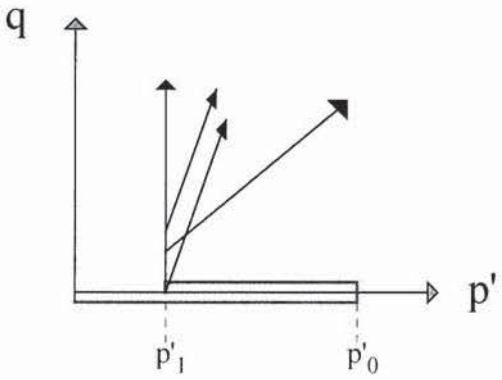

Fig. 2. Different stress paths combining deviatoric and isotropic loading

$$d\varepsilon_v^{(T)} = d\varepsilon_v^{(d)} \qquad (3)$$

The contribution of the isotropic part of the stress tensor on the volumetric strain mechanism was also studied along different stress paths for which the mean stress was not kept constant, as shown in Fig. 2.

TESTING PROGRAMM

Focusing on the stress-strain relationship and volumetric change measurements, the study required a reliable experimental system (especially for the volume change measurement), with an automatic recording system and test control.

As shown in Fig. 3, the system was made of various apparati connected by a closed loop. The test controls were operated by a PC via a driving program. Two acquisition (AC/DC) cards and an IEEE interface were integrated into the PC. Figure 3 also shows that the tests were conducted by using the hydraulic triaxial cell (Fig. 4). The radial stress noted σ_3 was applied by controlling the water pressure inside the cell, and the axial stress σ_1 was applied by controlling the pressure pr in the lower pressure chamber (Bishop and Wesley, 1975). The value of σ_1 is dependent on both σ_3 and pr following the

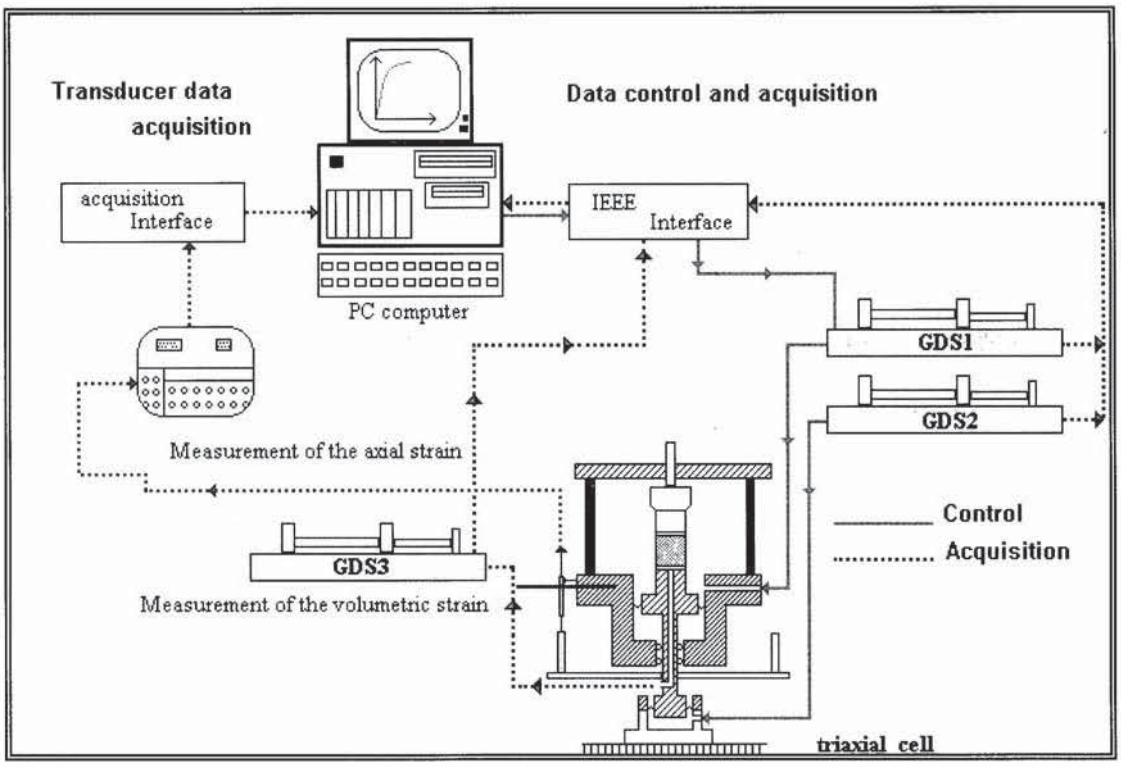

Fig. 3. Computer controlled hydraulic triaxial-testing system

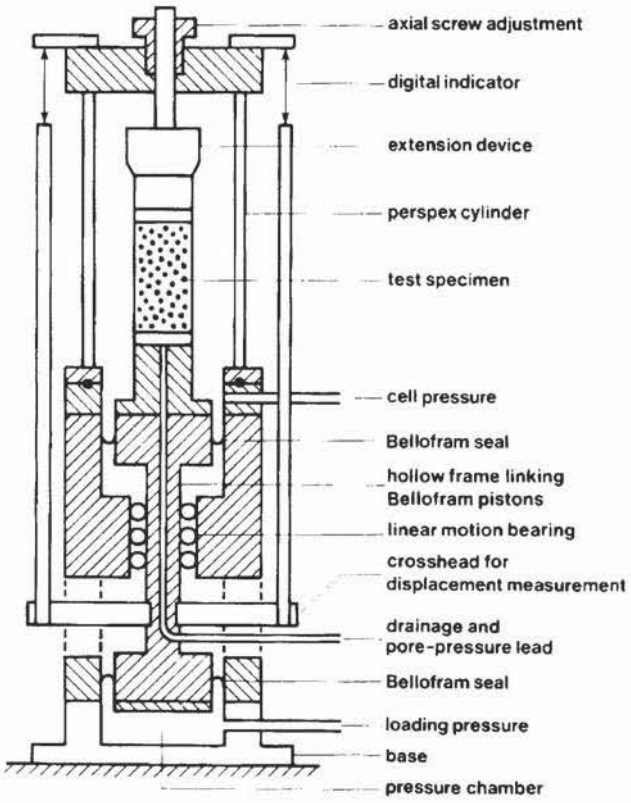

Fig. 4. Bishop's and Wesley's hydraulic triaxial apparatus

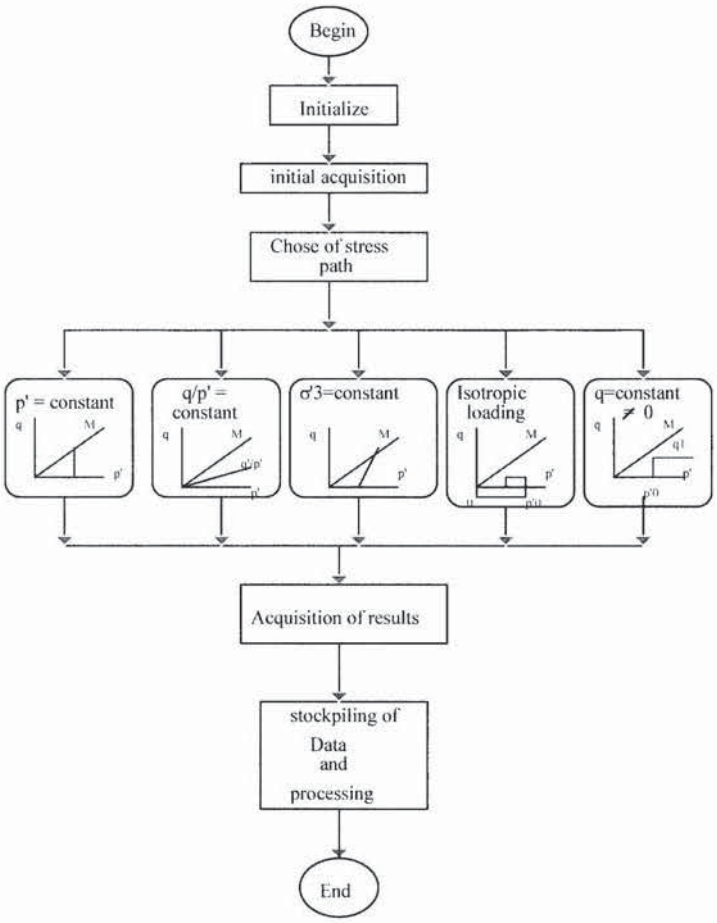

Fig. 5. Organisation chart of the driver program

relation (4):

Where:
$$\sigma_1 = pr\frac{a}{At} + \sigma_3\left(1 - \frac{a}{At}\right) - \frac{W}{At} \qquad (4)$$

At is the sample area
a is the bellofram seal area
W is the weight of the loading ram (located at the top of the pressure chamber)

This conception of the triaxial apparatus gave the possibility to control simultaneously pr and σ_3 so that we could follow different stress paths in loading as well as in unloading. This control was made by two controllers

Fig. 6(a). Procedure for applying a constant mean stress path

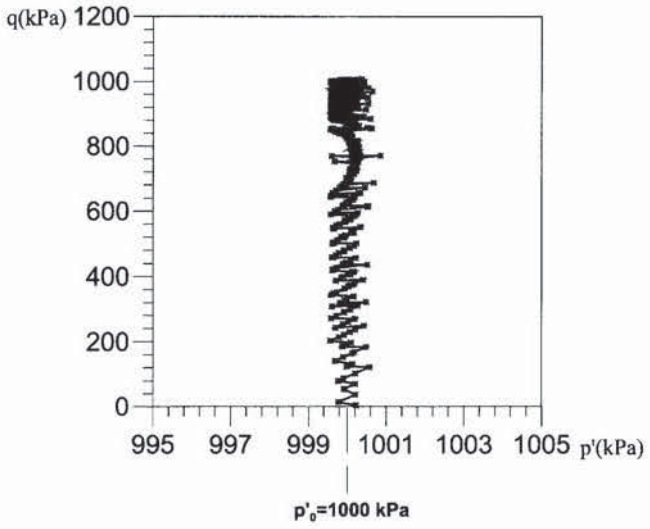

Fig. 6(b). Results of "constant mean stress path" procedure on a normally consolidated clay sample

(GDS1 and GDS2) via an IEEE interface. This operation is represented in Fig. 3 by a continuous line. The imposed stress values can be acquired at each moment for data processing. At the same time, we can calculate the deformations induced by the stress change, as represented in Fig. 3 by a broken line. As can be seen, the volume change was acquired by a third controller (GDS3) linked to the sample by a capillary tube. The axial displacement was measured by a LVDT transducer, the data being sent to the PC via the AC/DC interface.

This experimental environment was conducted by a software program called Piltriax (Hattab and Hicher, 1995). As an example, the classical path with σ_3 constant required only the control of pr. σ_3 was maintained constant and σ_1 was increased following the relation (5):

$$d\sigma_1 = \frac{a}{At}\, dpr \tag{5}$$

The "Piltriax" program insured the triaxial test control. The structure of its organization chart is represented in Fig. 5. The software was constructed so that it could be easy to add any other procedure to the five already implemented.

Another procedure example is "p' = constant" for the control of the triaxial test at a constant mean effective stress. The working principle consists of two steps, as explained in Fig. 6(a). The first step was to apply a pressure increment called pr. This step increased pr from p_0' to $pr1$. The second step was to bring p_1' back to p_0'. The pressure could be controlled with an accuracy of 1 kPa. This step required for relation (6) to be verified all along loading:

$$\sigma_1' + 2\sigma_3' = 3p_0' \tag{6}$$

Carrying out the "p' = constant" procedure allowed in obtaining a very good control of the stress path as shown by the example in Fig. 6(b). It corresponds to a constant mean stress path with $p' = p_0' = 1000$ kPa. We can note that, using this program, an accuracy of $dp' = \pm 1$ kPa was reached, which corresponds to the best use of the pressure controller GDS possibilities.

This experimental technique as a whole, considering the high degree of automation and of precision, allowed to investigate the mechanical behaviour of clay, following different stress controlled paths, and to obtain very reliable experimental results.

SPECIMEN PREPARATION

All the tests were performed on a remolded clay called "Kaolinite P300". Atterberg's limits were $L_L = 40\%$ and $P_L = 20\%$.

The specimen were prepared from a clay slurry mixed with a water content of twice the liquid limit and consolidated in a double drainage consolidometer at a vertical pressure of 120 kPa. After removing the sample, the specimens were trimmed and installed in the triaxial cell. The slenderness ratio (length to diameter) was chosen equal to 1 ($H = D = 35$ mm). An anti-frictional system was placed in the two extremities of the sample. The anti-frictional device was made of two circular smooth plates lubricated by means of a grease and latex layers 《sandwich》.

This kind of procedure was selected after considering the existing studies about the influence of the slenderness ratio and anti-frictional system on the strain homogeneity throughout the specimen (Hicher, 1985; Lade, 1985), and recently J.D. Frost and C.T. Yang (2003). The principal

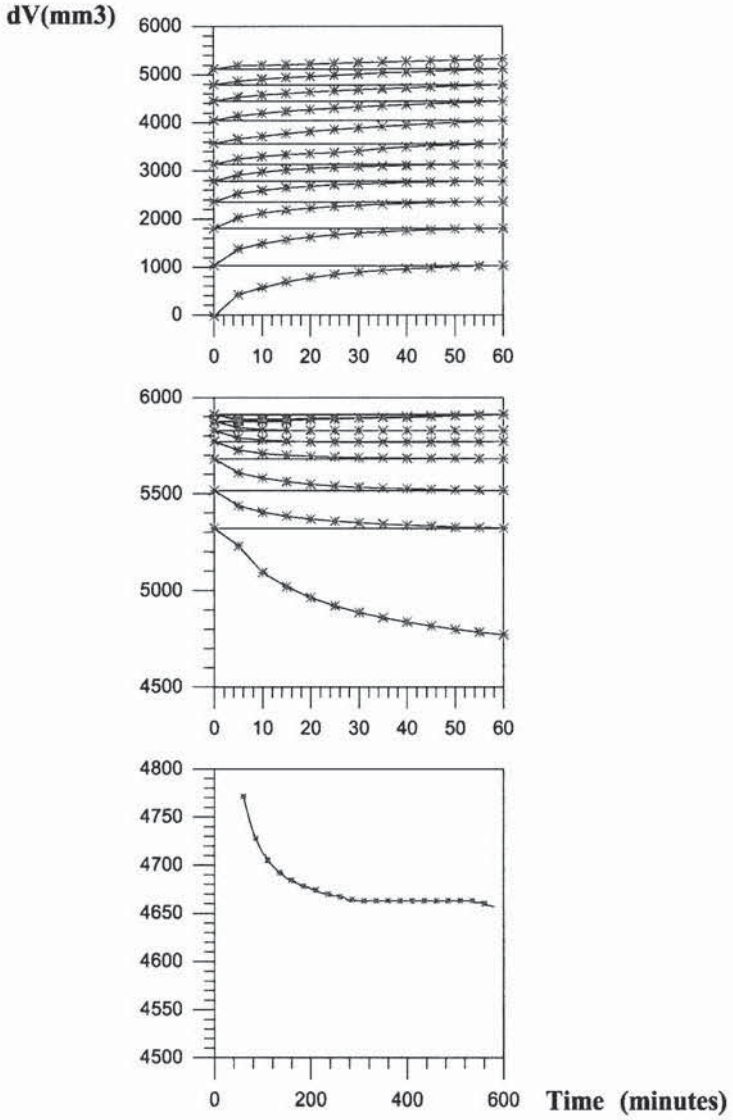

Fig. 7. Isotropic loading and unloading OCR = 8 and $p_0' = 1000$ kPa

purpose of the anti-friction system was to maintain the homogeneity of the sample up to large strains, by significantly reducing the friction at the sample ends. This allowed to reduce the slenderness ratio down to 1 and to prevent the rapid development of shear bands which are usually present in large strains, especially in overconsolidated clay.

BEHAVIOUR ALONG ISOTROPIC STRESS PATHS

In order to create initially a normally consolidated or overconsolidated state, the clay specimen were subjected to isotropic loading and unloading as represented in Fig. 1.

The specimen were isotropically loaded up to the maximum consolidation pressure $p_0' = 1000$ kPa, and then isotropically unloaded to the pressure $p_i' = p_0'/\mathrm{OCR}$, by degrees of 100 kPa/h, with volume changes recorded every 5 minutes, a similar operation mode for isotropic paths was previously performed by Shimizu (1982). Figure 7 shows an example of the isotropic consolidation of the clay with a final OCR of 8. This kind of consolidation process appears particulary interesting, because it ensures the detection of accidental leaks, particularly

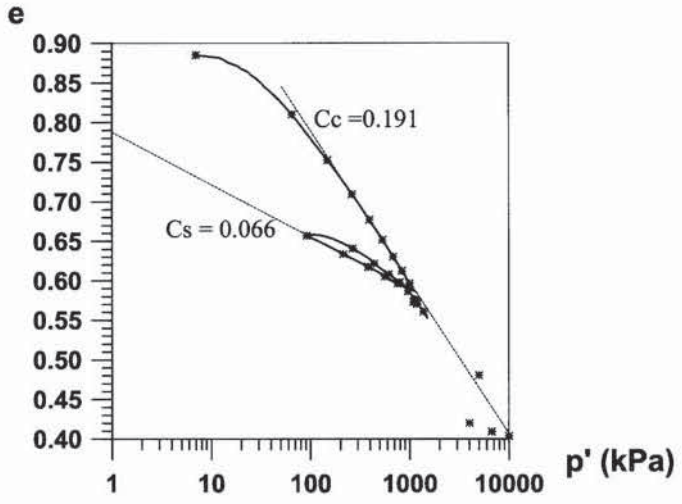

Fig. 8. Results of isotropic consolidation in e-p' plane

obvious in unloading, linked to an accidental porosity of the membrane. Since the volume changes were obtained by measuring the amount of pore water which circulated from and to the specimen, detecting accidental leakage through the membrane is highly significant. This approach imposed a very high level of precision in volume change measurements (Hattab and Hicher, 1995).

A series of 16 tests were performed on normally and overconsolidated clay samples with an OCR between 1 and 50 (Hattab, 1995). From the isotropic consolidation stages, values of the compression index $C_c = 0.19$ and of the swelling index $C_s = 0.066$ were measured. They both are usual values for a clay with low plasticity index (Fig. 8).

BEHAVIOUR ALONG PURELY DEVIATORIC STRESS PATHS

Figure 9 presents triaxial test results at constant mean stress in the planes (ε_1, q) and (ε_1, ε_v). For all tests, the maximum consolidation pressure was $p_0' = 1000$ kPa. The results show that the overconsolidation ratio influences not only the volumetric strain evolution with a dilatant behaviour for high OCR and a contractant one for low OCR, but also the strength evolution.

Evolution of the Maximum Strength q_{max}

In the (q, p') plane, normally consolidated clay samples are characterized by a maximum strength envelope corresponding to a straight line of slope $M = 1.05$. This line corresponds to a perfect plastic state also called critical state as defined in the Cam Clay model (Roscoe et al., 1958; Schofield and Wroth, 1968).

Overconsolidated clay samples with OCR > 2 are characterized by a maximum strength envelope corresponding to a curve called ζ which is situated above M (Fig. 10). The respective position of M and ζ indicates that the friction angle at peak is an increasing function of OCR (Fig. 10). This maximum strength envelop ζ can be consider as a precise representation of Hvorslev surface in the (p'-q) plane. It is not a straight line as proposed by Parry (1960).

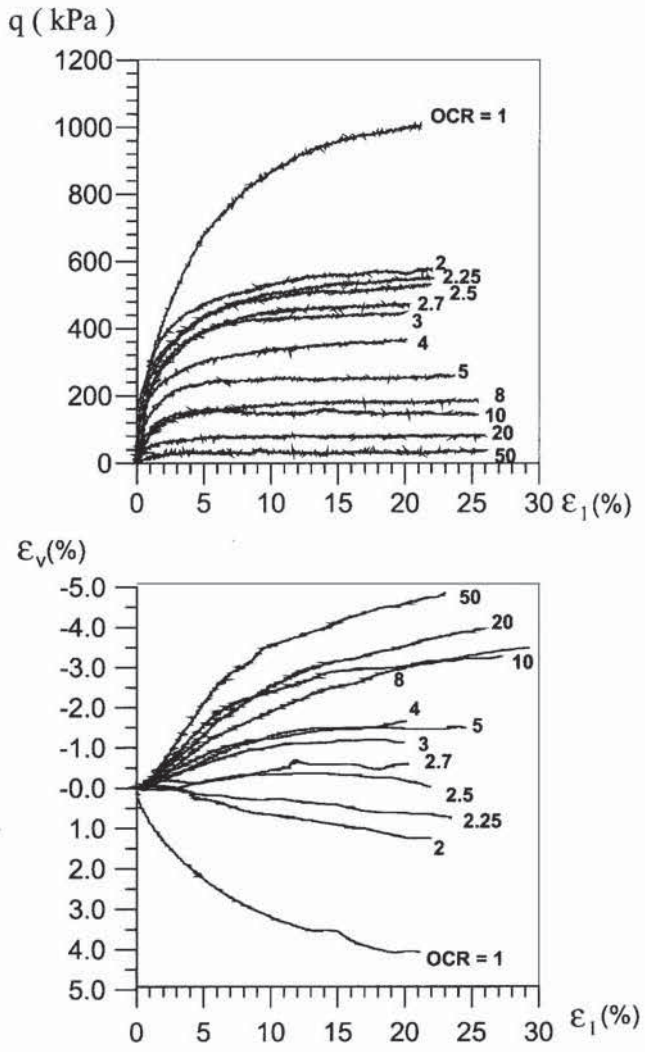

Fig. 9. Constant mean stress tests on clay samples with different OCRs

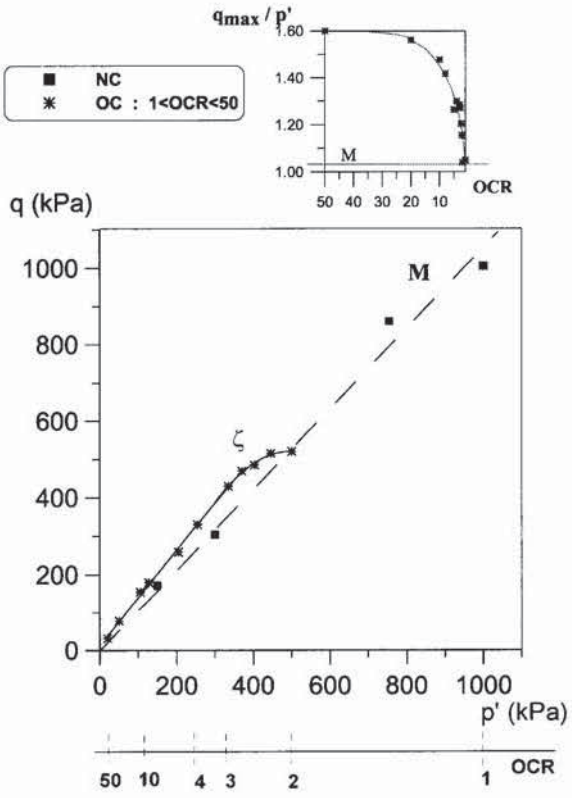

Fig. 10. Maximum strength envelops in constant mean stress paths with different OCRs

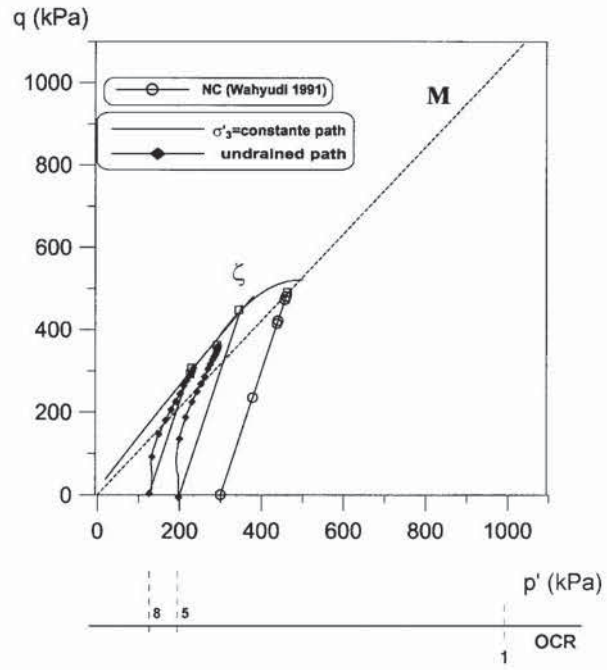

Fig. 11. Maximum strength envelops in σ'_3 = constant paths with different OCRs

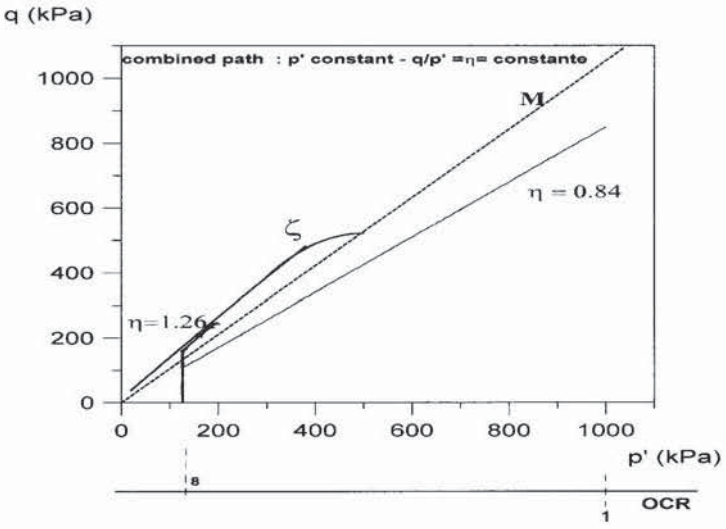

Fig. 12. Combined stress paths on OCR = 8 clay sample

The ζ and M curves remain valid for other axisymmetric stress paths, as the conventional triaxial tests (σ_3 = constant). In Fig. 11 drained test results by Wahyudi (1991) on normally consolidated samples giving the same value of M are presented. In the same figure, drained and undrained triaxial tests with OCR = 5 and 8 end up on the ζ envelope.

Figure 12 presents the results of more complex paths constituted by two parts: the first part corresponds to a constant mean stress loading and the second part to a $\eta = q/p'$ = constant stress path. One can see that, for OCR = 8 and $\eta = 1.26$, a maximum strength q_{max} located on the ζ curve is obtained. For $\eta = 0.84$ lower than M, loading can be continued without any occurrence of the sample failure.

Most of the tests were performed at the same maximum isotropic consolidation stress = 1000 kPa. Few others

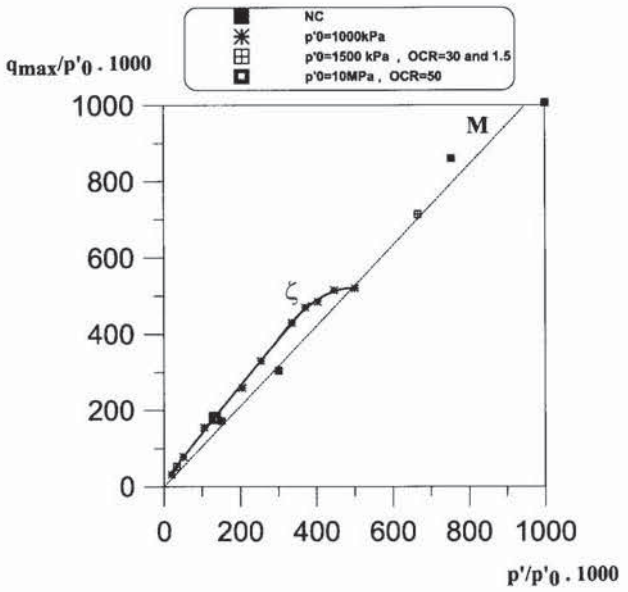

Fig. 13. Strength envelop normalized by the preconsolidation pressure

were performed at higher values of p_0'. We can add to the previous tests the following test results at constant mean stress so that:

OCR = 30 and 1.5 $\quad p_0' = 1500$ kPa

OCR = 50 $\quad p_0' = 10$ MPa

In order to investigate the influence of p_0' on the results, all the tests were plotted in an adapted plane (q_{max}/p_0', p'/p_0'), (Fig. 13). One can see that for OCR = 50 and 30, the stress paths end on the same ζ line. For OCR = 1.5, the maximum strength is located on the same straight line M. For higher consolidation pressures, the line M is probably no longer straight, there is a decrease in the slope as shown by Biarez and Hicher (1994).

Thus, the two curves ζ and M are intrinsic characteristics of the clay. It represents, in the plane (p', q), the boundaries which delimit the size of the domain accessible by different loading paths. Clay behaviour inside this domain will be analyzed below.

Volumetric Strain Evolution

The volumetric strain evolution was investigated mainly in the (e, p') plane. The evolution of the void ratio e, for normally consolidated clay samples during constant p' and constant σ_3' loading is presented in Fig. 14(b). Isotropic loading (C_c) and unloading (C_s) are also plotted on this plane. We can note here that the points representing the end of loading are located on a straight line, parallel to the isotropic consolidation line (C_c). Since the volumetric strain reached a constant value for large deformations, this line corresponds to a perfect plastic state (or critical state). This remains valid for all OCRs apart from two cases: OCR = 50 and 20 as it appears in Fig. 14(a). In these two last cases, we can observe in Fig. 9 that the volumetric strain at the end of the test was not stabilized. We can therefore assume that the perfect plastic state was not reached.

The perfect plastic line cuts the isotropic unloading line

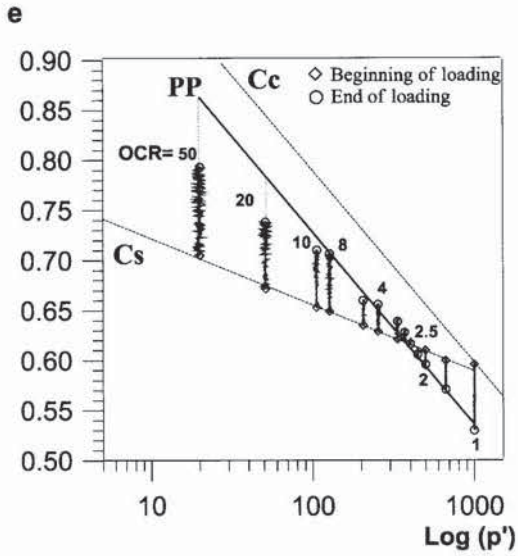

(a) Constant mean stress paths with different OCRs

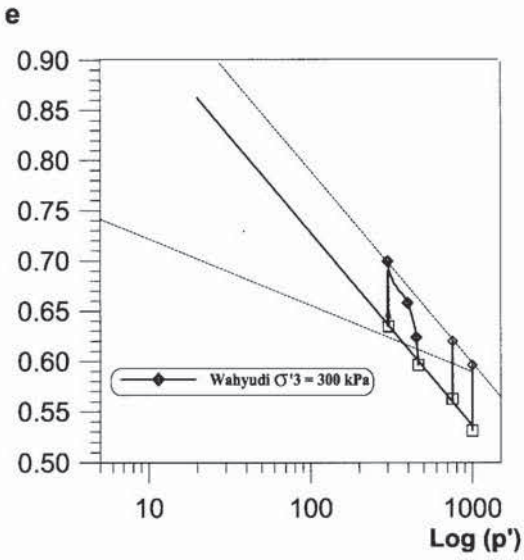

(b) Constant mean stress and constant σ_3' paths for NC samples

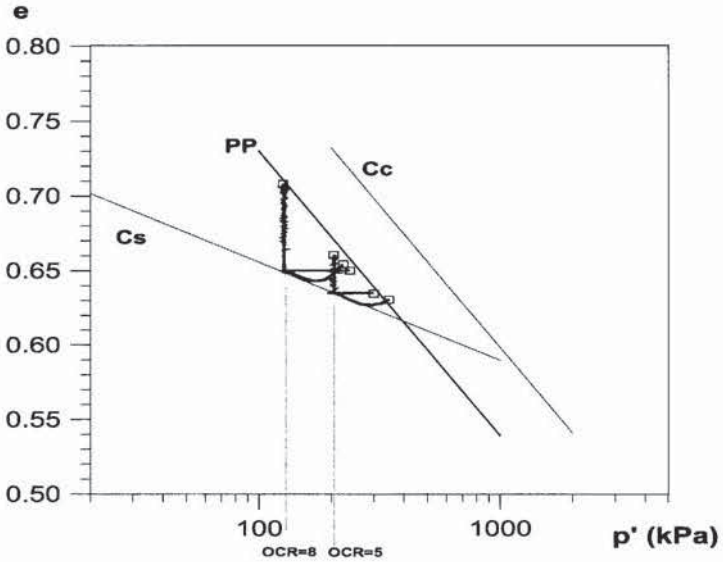

(c) Constant mean stress and constant σ_3' paths for OC samples

Fig. 14. e-p' evolution for different stress paths

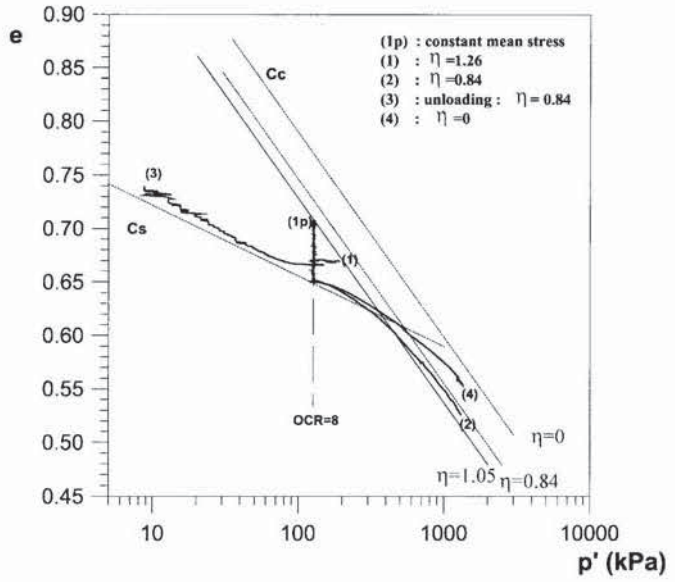

Fig. 15. e-p' relationship for overconsolidated clay samples

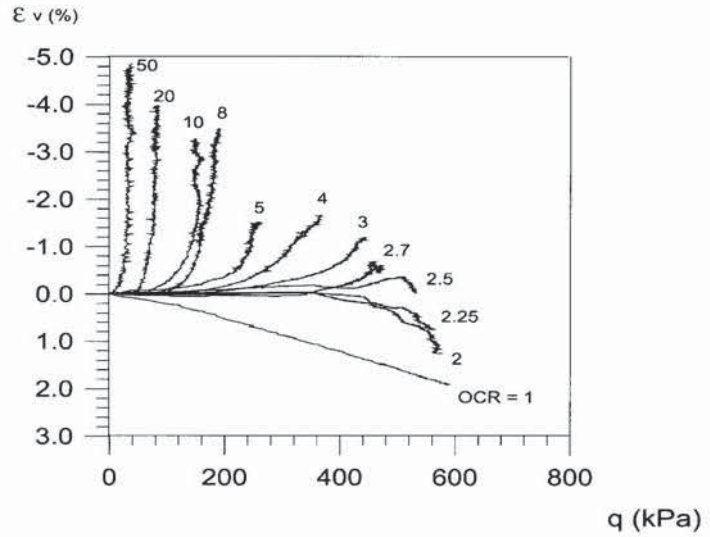

Fig. 16. Volume changes as function of deviatoric stress in constant mean stress tests

for OCR = 2.5. In these conditions for OCRs < 2.5, the clay sample exhibits a decrease of the void ratio during a constant p' loading, corresponding to a contractant behaviour, while for OCRs > 2.5 the samples present an increase of the void ratio, corresponding to a dilatant behaviour.

In Fig. 14(c), the results obtained for two OCRs are presented: 8 and 5, for p' = constant and σ_3' = constant loading paths as well as for undrained tests. We can see that the same perfect plastic line is obtained for all the tests. The p' constant tests and undrained tests are represented, respectively, by vertical and horizontal straight lines, whereas σ_3' = constant tests follow, at first, the reloading line (C_s) and, after a certain point, leave this line to exhibit a dilatant behaviour up to the perfect plastic line. These results will be analyzed later in terms of plastic mechanisms.

Several more complex loading paths were applied on samples overconsolidated at OCR equal to 8 (Fig. 12). The behaviour can be observed in Fig. 15, where, **(1p)**, **(1)**, **(2)**, **(3)** and **(4)** correspond to the following stress paths:

(1p) is a constant mean stress path as already discussed before.

(1) is a stress path combining different loading stages: at first a constant mean stress path beyond the perfect plastic line M, and then a constant $\eta = q/p' = 1.26$ path up to failure. In Fig. 12 one can see that this path has reached the ζ curve. In the (p', e) plane (Fig. 15), the path followed, during the first part of the test, a vertical line towards the increasing values of e and then, during the second part of the loading, reached the perfect plastic line with no volume change (e = constant).

(2) is the same path as in the case **(1)**, i.e. the stress path combines a first part at constant mean stress and a second part at constant $\eta = 0.84$ in which the maximum strength envelop ζ or M is never reached. In the (p', e) plane, the corresponding path reached a line parallel to the isotropic consolidation line and the perfect plastic state line, located between these two lines. This line corresponds to the locus of the points corresponding to $\eta = 0.84$ in normally consolidated tests.

(3) is a constant mean stress up to $\eta = 0.84$ followed by an unloading test with η = constant = 0.84. In the (e, p') plane, the path obtained during the unloading part reached the C_s line and then followed it until the end of the test.

(4) is an isotropic loading path. In the (e, p') plane it corresponds to a classical consolidation line following at first a line of slope C_s and then a line of slope C_c when a normally consolidated state was obtained.

All these results allow to characterize the perfect plastic state, defined by the perfect plastic line in the (e, p') plane. This straight line is parallel to the isotropic line C_c. Besides, one can define a domain of dilatancy for high OCRs and a contraction domain for low OCRs. OCR = 2.5 (where no volume change was observed during a p' constant path) is, for the studied clay, the point where a change takes place between the two behaviour areas. In the dilatant domain, the relation e-p' is governed, at small stress ratios, by the line C_s which is followed along stress paths corresponding to either an increase or a decrease of the mean stress p'. For higher stress ratios, the dilatant behaviour will superimpose its influence on this general trend.

CHARACTERIZING DILATANCY ALONG CONSTANT MEAN STRESS LOADING

In the (q, ε_v) plane, we can study the volumetric strain evolution as a function of the deviatoric stress for different OCRs (Fig. 16). For OCR values between 1 and 2.5 we observe a contractant behaviour, while a dilatant behaviour characterizes all the specimen with OCR > 2.5. The maximum slope defined by $(\varepsilon_v/q)_{max}$ is an increasing function of OCR. Dilatant behaviour for OCR greater than 2.5 or contractant behaviour for OCR smaller than 2.5 starts after an initial no-volume phase, except for

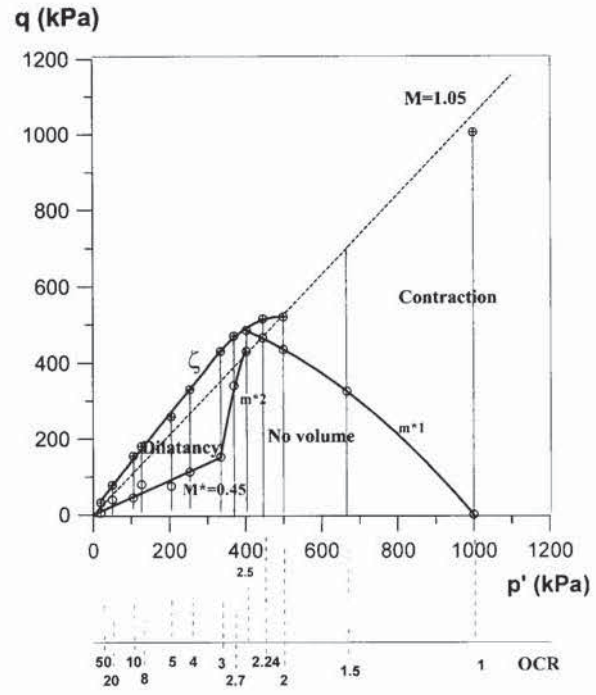

Fig. 17. Volume change condition in the (p', q) plane

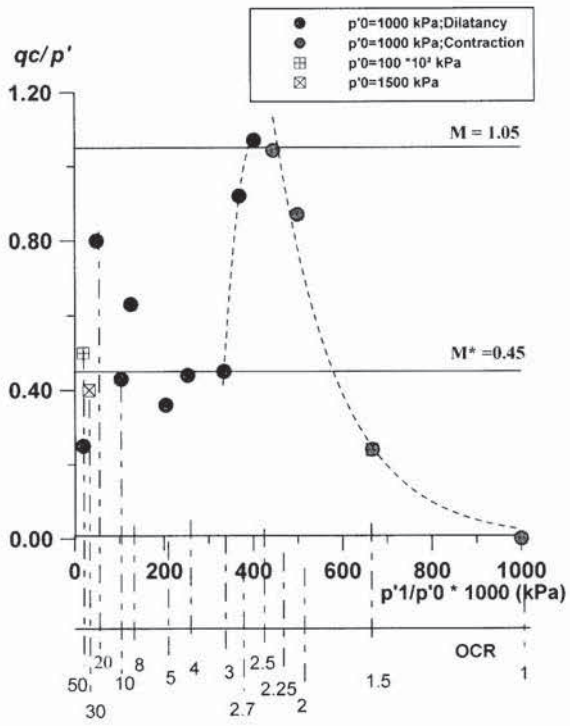

Fig. 18. Stress conditions corresponding to the beginning of volume change for different OCRs

OCR = 1 which shows a contractant behaviour since the beginning of the loading.

We called q_c the deviator which started to induce a volumetric strain, positive or negative, after the no-volume phase. If we report the corresponding points in the plane (p', q), we obtain several domains (Fig. 17). The dilatancy domain is obtained for high OCRs (OCR $\geq$ 2.5) and is limited by the maximum strength envelope; the contraction domain for low OCRs (OCR $\leq$ 2.5) is limited by the critical state line M. These two domains are limited by a third domain of no volume change. The boundaries of this third domain correspond to the beginning of dilatancy or contraction and can be defined by M^*, m^*_2 and m^*_1. This result is in agreement with a similar zone, defined like a nucleus within which only elastic volumetric strains take place, proposed by Balasubramaniam et al. (1993). However, this zone seems to be more reduced than the no volume change domain obtained in Fig. 17. Tests were carried out on overconsolidated soft Bangkok clay which more submitted to a variety of stress paths.

M^* is a straight line for OCR $\geq$ 3. Its slope is equal to 0.45 and it is located underneath the critical state line M (equal to 1.05) (Fig. 17).

For OCR between 2.5 and 3, there is a transition behaviour and the locus of the stress states characterizing the beginning of dilatancy is a curve called m^*_2 which connects the M^* line and the ζ curve.

For OCR lower than 2.5, we obtain a curve m^*_1 characterizing the beginning of contraction. The shape of this curve is similar to the yield surface in Cam Clay Model.

We can see in Fig. 18 that we obtain for high OCRs a scattering in the values of q_c/p' around the M^* line. These results are due to the small initial stress values for the highest OCRs. For this purpose, we performed some other tests with a higher value of the maximum consolidation stress p'_0. Therefore, the mean stress p'_1 for a given OCR is also increased (for example $p'_1 = 200$ kPa, OCR = 50). In these conditions we obtained an experimental point q_c/p' closer to M^*.

PLASTIC FLOW ANALYSIS

Having defined the conditions by which the maximum strength develops and how the dilatancy evolves according to the overconsolidation ratio, we will now study the conditions of development of plastic strains, and mainly the evolution of the ratio between the plastic volumetric strain increment $d\varepsilon^p_v$ and the plastic deviatoric strain increment $d\bar{\varepsilon}^p$ which gives the condition of plastic flow along triaxial stress paths.

Dilatancy in Cam Clay Model

The Cam Clay Model was developed in the 1960s by Roscoe et al. (Roscoe et al., 1958; Schofield and Wroth, 1968). The model is based on elastoplasticity concepts and on the clay behaviour in triaxial compression tests.

Equation (7) gives the flow rule:

$$M - \frac{q}{p'} = \frac{d\varepsilon^p_v}{d\bar{\varepsilon}^p} \tag{7}$$

The perfect plastic state, called critical state was introduced:

$$d\varepsilon^p_v = 0 \quad \text{and} \quad M - \frac{q_c}{p'_c} = 0 \tag{8}$$

Relation (7) is compatible with a plastic potential function such as:

With:

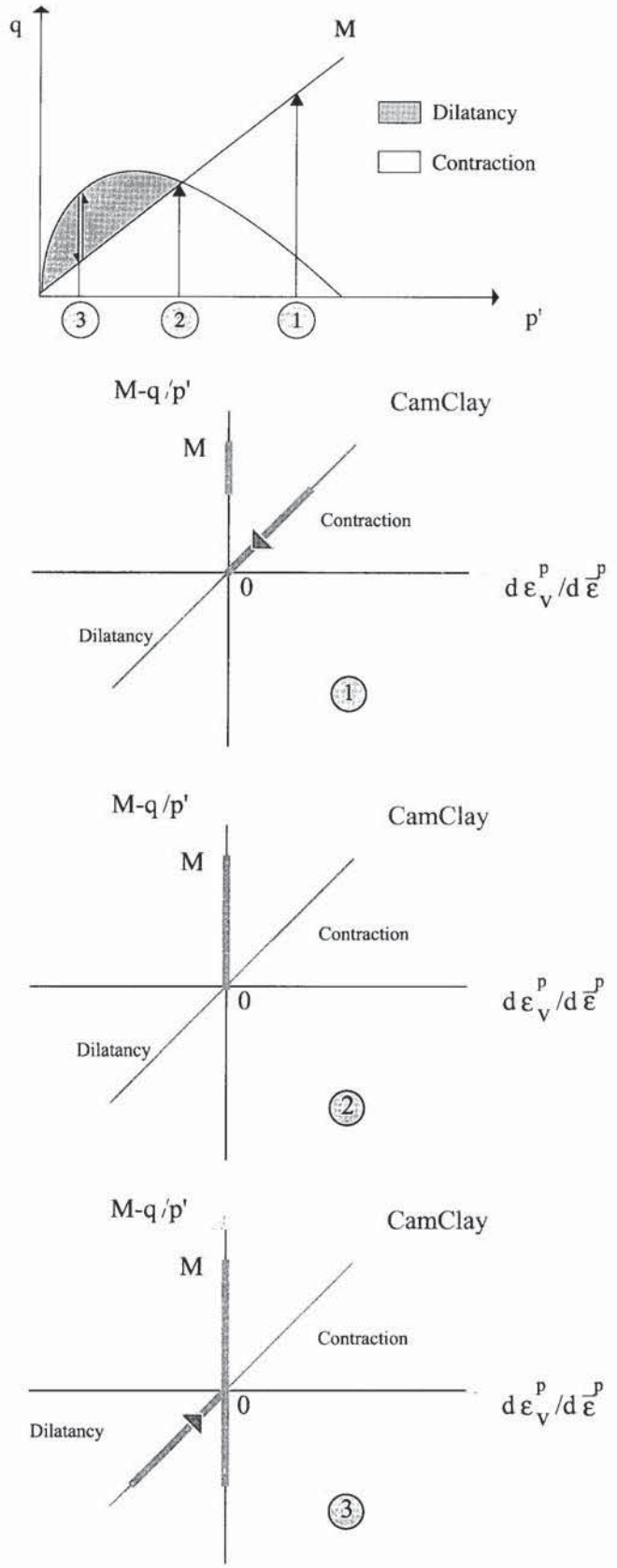

Fig. 19. Plastic flow in Cam Clay model

$$g(p', q) = \frac{q}{Mp'} + \ln \frac{p'}{p'_{ic}} \qquad (9)$$

$d\varepsilon_v^p$ →plastic volumetric strain increment
$d\bar{\varepsilon}^p$ →plastic deviatoric strain increment
p'_{ic} →consolidation pressure

$\frac{q_c}{p'_c}$ →invariant stress ratio at critical state

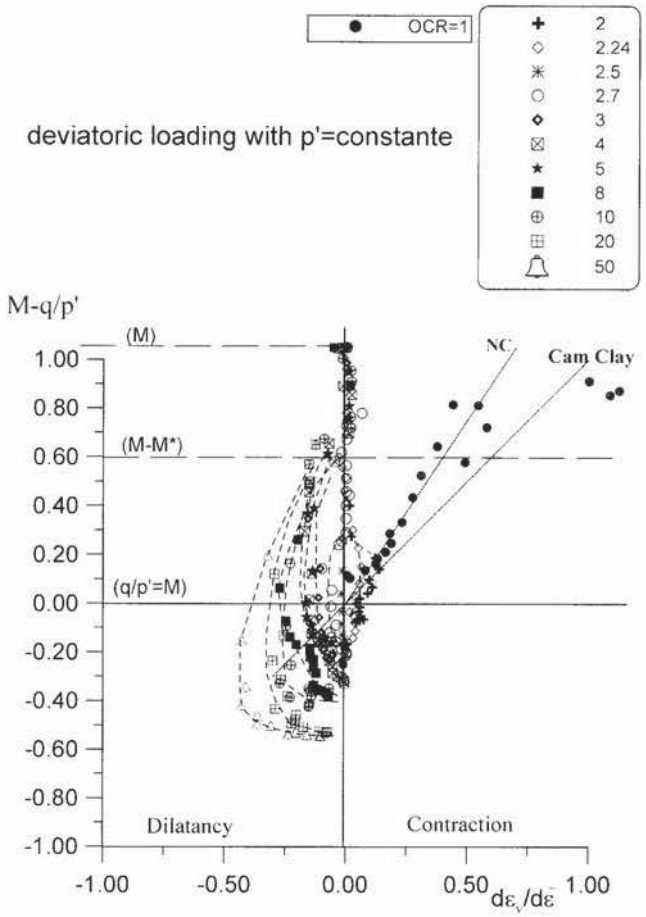

Fig. 20. Plastic flow during constant mean stress tests at different OCRs

Figure 19 shows the plastic flow in the Cam Clay model, for three different initial states in the $(d\varepsilon_v^p/d\bar{\varepsilon}^p, M-q/p')$ plane.

1. A slightly overconsolidated clay called "wet clay". The beginning of loading is elastic ($d\varepsilon_v^p = d\bar{\varepsilon}^p = 0$). Then, a plastic contraction is induced following a straight line with slope = 1, before reaching the perfect plastic state for $M\text{-}q/p' = 0$.

2. The intermediate state, obtained for OCR = 2.7. The perfect plastic state follows the elastic behaviour immediately: we obtain an elastic, perfectly plastic behaviour.

3. For higher OCRs the behaviour is at first elastic until the maximum strength is reached, corresponding to the actual position of the yield surface. Later dilatancy appears following a straight line with slope = 1, its development evolves with a decrease of the deviatoric stress until the plastic perfect state is reached.

Plastic Flow during Constant Mean Stress Paths for Different OCRs

We found that the plastic flow occurred differently according to the overconsolidation ratio. The analysis was conducted in the $(d\varepsilon_v^p/d\bar{\varepsilon}^p, M-q/p')$ plane (Fig. 20).

For normally consolidated samples, the plastic flow follows a straight line in this plane. It can be defined by:

$$M - \frac{q}{p'} = \alpha \cdot \frac{d\varepsilon_v^p}{d\bar{\varepsilon}^p} \qquad (10)$$

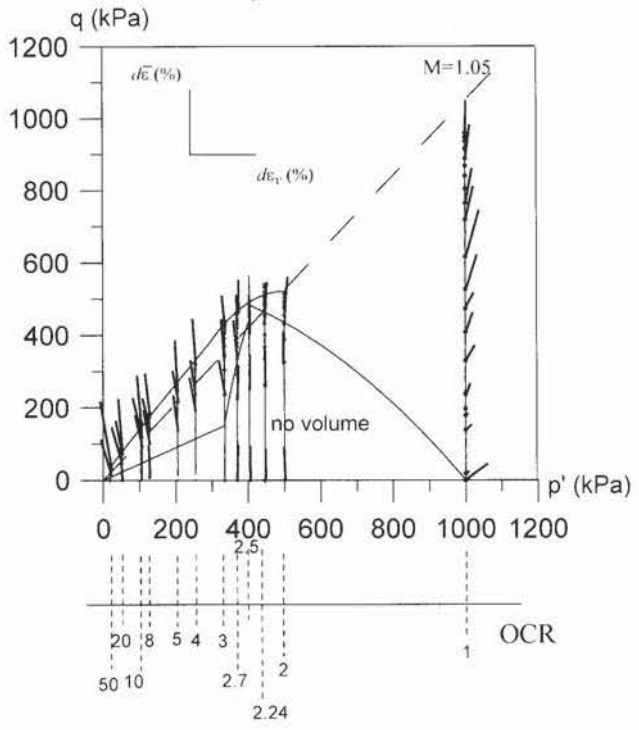

Fig. 21. Evolution of plastic strain increment directions during constant mean stress tests

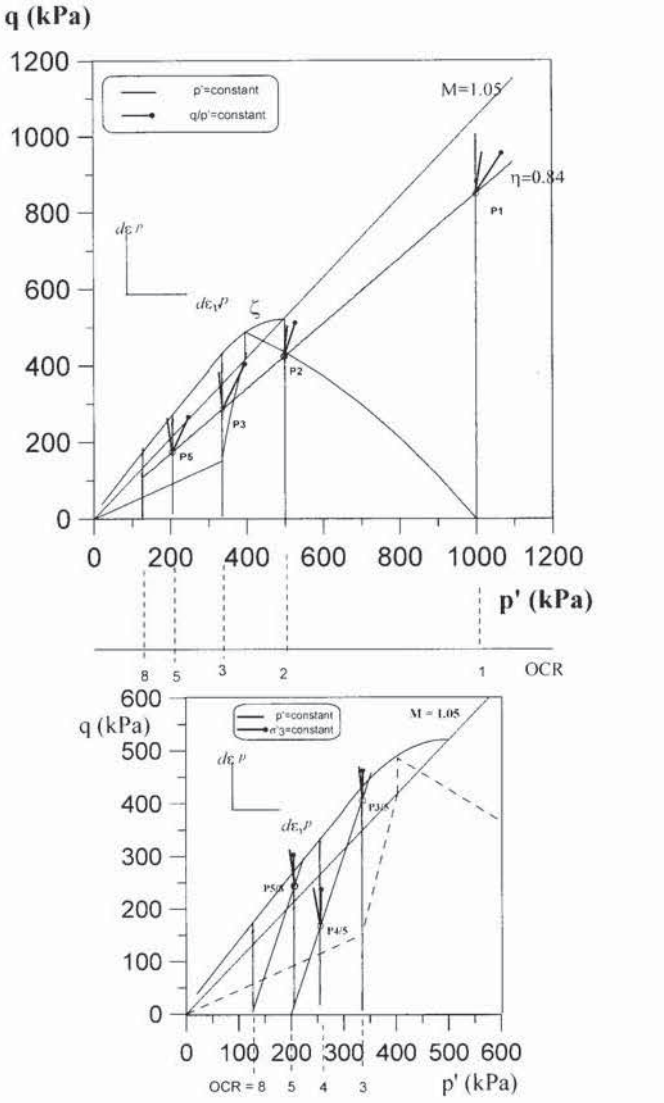

Fig. 22. Influence of stress increment direction on plastic strain increment direction at concourse points

where $\alpha = 1.5$.

We obtain therefore a plastic flow rule slightly different from the one assumed in the Cam Clay model where α is equal to 1.

As one can see in Figs. 20 and 21 for overconsolidated samples, plastic flow is dependant entirely on the OCR values. For all OCRs, a plastic volumetric flow equal to 0, was observed in the beginning of each loading. The limit of this first phase corresponds, in (p', q) plane to the straight line M^* for OCR ≥ 3, to the curve m^*_2 for OCR $= 2.7$ and 2.5, and to the curve m^*_1 for OCR $= 2$ and OCR $= 2.24$ (Fig. 17). We obtained a similar shape of the elastic domain as the one assumed by the Cam Clay model in the case of small OCRs (OCR $= 2$, and OCR $= 2.24$) as we can see in case 1, Fig. 19, and also for OCR $= 2.5$ for which we noted that $d\varepsilon_v^p$ was equal to 0 all along the loading; this corresponds for the Cam Clay model to case 2 (Fig. 19).

For OCR ≥ 3, Cam Clay Model assumes that the material behaves elastically ($d\varepsilon_v^p = 0$) until the yield surface is reached beyond M (Fig. 19, case 3). In our experiments, the plastic flow was obtained earlier, for M-$q/p' = 0.6$ as we can see in Figs. 20 and 21.

If we analyze now how the plastic flow develops when $d\varepsilon_v^p/d\bar{\varepsilon}^p \neq 0$, we can see in Figs. 20 and 21 that:

1— For OCRs ≥ 2.5, the dilatancy rate, defined by the value of $d\varepsilon_v^p/d\bar{\varepsilon}^p$ first increased up to a certain stress ratio and then decreased to 0. This stress ratio is an increasing function of the OCR and is equal to 0 for OCR $= 2.5$, in agreement, for this last point, with the Cam Clay Model as we discussed before (Fig. 19, case 2).

2— For OCRs < 2.5 we can observe that the volumetric plastic flow occurred following two stages of contractancy: the first one corresponds to an increase of $d\varepsilon_v^p/d\bar{\varepsilon}^p$ and the second one to a decrease of $d\varepsilon_v^p/d\bar{\varepsilon}^p$. The Cam Clay model seems agree in this case.

These results confirm the fact that the Cam Clay model can simulate correctly the behaviour of slightly overconsolidated clays (OCR < 2 to 3) but is far from reality for higher OCRs.

Study of Stress Path Influence on Plastic Flow Phenomenon

Given one stress state located within either the dilatant or the contractant domain, the application of a stress increment $d\sigma'$, defined by dq and dp' induces a plastic strain increment $d\varepsilon^p$ defined by $d\varepsilon_v^p$ and $d\bar{\varepsilon}^p$. We will examine here the influence of the initial stress state and of the stress increment on the orientation of the plastic increment given by the ratio $d\varepsilon_v^p/d\bar{\varepsilon}^p$. The first point concerns the evolution of the plastic strain increment direction as a function of the stress increment direction. Thus we will investigate it in seven concourse points following different stress paths. As we can see in Fig. 22, P5/8, P4/5, and P3/5 are concourse points in (p', q) plane between p' constant and σ_3' constant stress paths. P5, P3, P2, and P1 are concourse points between a path

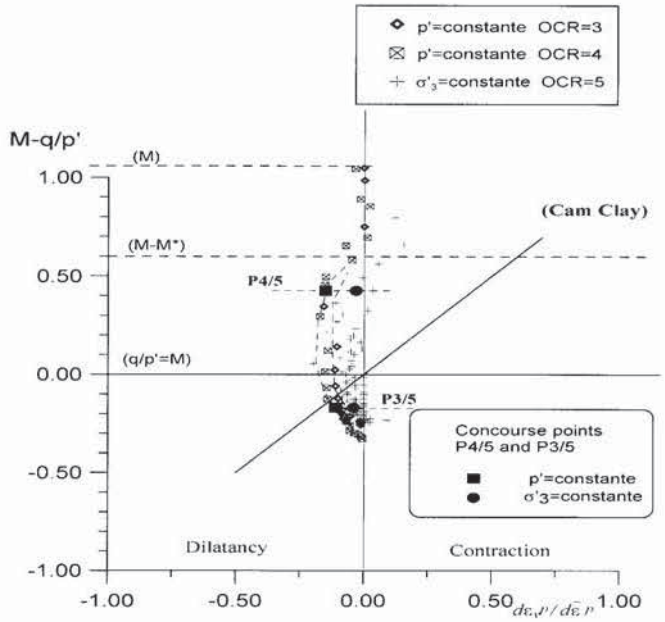

Fig. 23. Plastic flow evolution along different stress paths for OCR = 5 clay sample

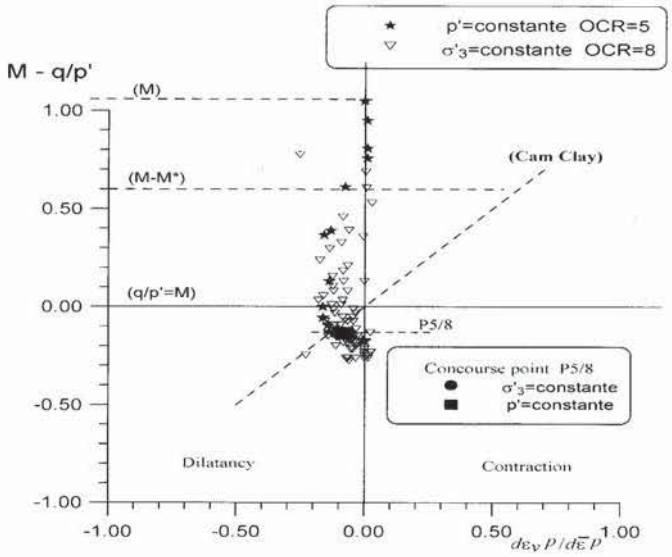

Fig. 24. Plastic flow evolution along different stress paths for OCR = 8 clay sample

at $\eta = q/p'$ constant and different p' constant paths (Fig. 22).

On stress paths where a change in the mean effective stress p' occurred, plastic volumetric strain increment were measured by using Eq. (2). $d\varepsilon_v^{(d)}$ was assumed to be purely plastic, while $d\varepsilon_v^{(i)}$ was assumed to be purely elastic for overconsolidated specimens. $de^{(i)}$ could be calculated from the relation between e (void ratio) and p'(mean effective stress), obtained from isotropic unloading (Fig. 8).

From where:

$$de^{(i)} = \frac{C_s}{2.3}\frac{dp'}{p'} \tag{11}$$

or:

$$d\varepsilon_v^{(i)} = \frac{C_s}{2.3\ (1+e_0)}\frac{dp'}{p'} \tag{12}$$

The concourse points P1, P2, P3 and P5 show clearly the dependency of $d\varepsilon_v^p/d\bar{\varepsilon}^p$ with the stress increment directions (Figs. 22 and 25). In points P5 and P3 (Fig. 22) the two vectors $d\varepsilon^p$ are located on both sides of the vertical direction, which means plastic dilatancy for $p' = \text{const}$ path and plastic contraction for $\eta = \text{const}$ path. In points P1 and P2, the directions of the plastic strain increments are located on the same side of the vertical direction (Fig. 22). However, the directions are clearly different. From these results, we can conclude that, when the directions of $d\sigma'$ at a given stress point are significantly different (P1, P2, P3, P4), we clearly obtain different orientations of plastic strain increments. Therefore, the uniqueness of the plastic potential cannot be verified.

In P4/5 case we can note a small difference, the stress path direction seems to influence here also the value of $d\varepsilon_v^p/d\bar{\varepsilon}^p$ (Figs. 22 and 23). In this case the directions of $d\sigma'$ are closer, which lead to also closer directions for the strains increments compared to the results presented

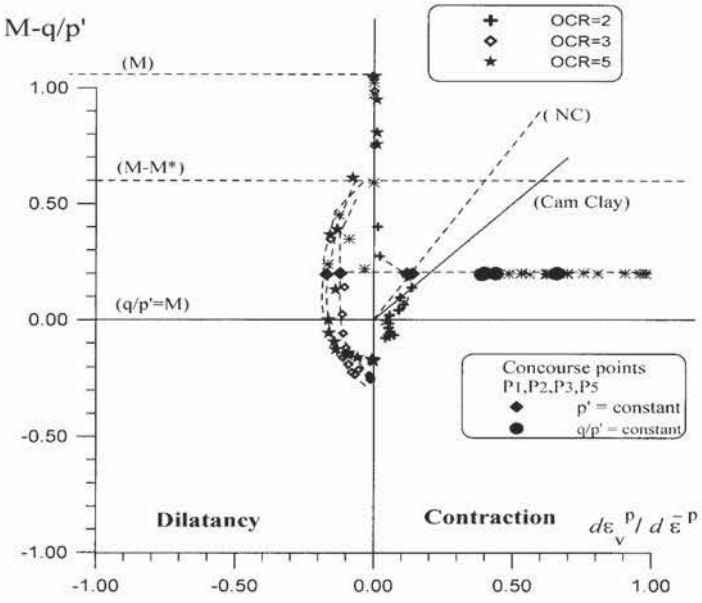

Fig. 25. Plastic flow evolution along two different stress paths for several OCRs

above.

For points P5/8 and P3/5, $d\varepsilon_v^p/d\bar{\varepsilon}^p$ is practically identical for the two loading paths (Fig. 22). When the stress points approach the straight line M, the plastic volumetric strain increment is close to zero for any stress path, which indicates that the plastic potential can be considered as unique (Figs. 23 and 24). This shows that the hypothesis which is often assumed (e.g. Pender, 1978) that the direction of the stress path has a slight effect on the direction of the plastic strain increment vector, is not always verified.

The results presented above along constant mean stress paths allow to define a deviatoric plastic mechanism which is induced by a purely deviatoric stress increment. The introduction of an isotropic stress component, using different loading paths, shows that the unicity of the

plastic potential is not verified. We observe a combined effect of two mechanisms: a deviatoric type mechanism due to the deviatoric part of the stress tensor, and an isotropic type mechanism due to the isotropic part of the stress tensor. By combining these two effects, we obtain, at a given stress point, an influence of the stress increment vector direction on the plastic flow as indicated in Figs. 23 and 24. In particular, the dilatancy rate due to the deviatoric loading can be modified by the amplitude of the isotropic stress increment, and therefore, the dilatant behaviour of a clay specimen depends strongly on both the overconsolidation ratio and the loading path.

CONCLUSION

The initial state of a clay sample can be characterized by its overconsolidation ratio. It is a very important parameter which controls the amount of volumetric strain during loading. When subjected to a pure deviatoric loading, overconsolidated samples dilate after having reached a given value of the deviatoric stress, whereas a normally consolidated or a slightly overconsolidated sample is always contractant.

The analysis of the clay behaviour undertaken in this study, highlighted some mechanical characteristics suitable for all the stress paths investigated above. These parameters control the relationship between void ratio and mean effective stress and correspond to the slopes of the one-dimensional consolidation and swelling lines (C_c and C_s), as well as the positions of the one-dimensional compression line and the perfect plastic line (*PP*) in the (e-log p') plane. A second set of parameters control the boundaries of the domain in the stress plane (p'-q). M corresponds to the slope of the perfect plastic line in this plane and ζ represents the envelop of peak strength above the perfect plastic line for overconsolidated samples. Inside these upper boundaries, the stress plane can be divided into different regions corresponding to a contractant, dilatant or no-volume change behaviour along pure deviatoric stress paths.

The study of the plastic flow inside these different regions leads to the following conclusions. In the contractant domain, the plastic flow represented by the ratio $d\varepsilon_v^p/d\bar{\varepsilon}^p$ follows a relationship close to the one proposed by the Cam Clay model:

$$M - \frac{q}{p'} = \alpha \cdot \frac{d\varepsilon_v^p}{d\bar{\varepsilon}^p} \quad \text{with } \alpha = 1.5$$

For highly overconsolidated samples, the dilatancy appears for a value of the stress ration q/p' smaller than M and the plastic strain ratio $d\varepsilon_v^p/d\bar{\varepsilon}^p$ increases first up to a maximum value and then decreases to 0 when the perfect plastic state is reached.

The constant mean stress path generates a plastic strain mechanism due to a pure deviatoric stress increment. When an isotropic stress part is introduced using different loading paths, the unicity of the potential cannot be verified. The results show a combined mechanism effect: a deviatoric mechanism and an isotropic mechanism, these two kinds of mechanism are strongly dependent and lead to a dependency of the plastic strain increment vector with the direction of the stress increment. When the stress point comes close to the perfect plastic state, the plastic potential can be considered as unique.

REFERENCES

1) Asaka, Y., Tokimatsu, K., Iwasaki, K. and Shamoto, Y. (2003): A simple stress-strain relation based on stress-path behavior in strain-path controlled triaxial tests, *Soils and Foundations*, **43** (2), 55–68.
2) Balasubramaniam, A. S., Kim, S. R. and Honjo, Y. (1993): Formulation of stress-strain behaviour inside the state boundary surface, *Proc. 11th Southeast Asian Geotechnical Conference*, Singapore, 3–14.
3) Biarez, J. and Hicher, P. Y. (1994): *Elementary Mechanics of Soils Behaviour, Saturated Remoulded Soils*, A. A. Balkema, Rotterdam, Brookfield.
4) Bishop, A. W. and Henkel, D. J. (1962): *The Measurement of Soil Proprieties in the Triaxial Test*, Edward Arnold, London.
5) Bishop, A. W. and Wesley, L. P. (1975): A hydraulic triaxial apparatus for controlled stress path testing, *Géotechnique*, **25** (4), 657–670.
6) Frost, J. D. and Yang, C. T. (2003): Effect of end platens on microstructure evolution in dilatant specimens, *Soils and Foundations*, **43** (4), 1–11.
7) Hattab, M. (1995): Etude expérimentale du comportement dilatant des argiles surconsolidées, *Thèse de doctorat Ecole Centrale Paris Chatenay-Malabry* (in French).
8) Hattab, M. and Hicher, P. Y. (1995a): Experimental study of the dilatancy in overconsolidated clay, *Proc. International Symposium on Compression and Consolidation of Clayey Soils Is-Hiroshima '95*, Japan, A. A. Balkema, Rotterdam, Brookfield, 1995, 57–62.
9) Hattab, M. and Hicher, P. Y. (1995b): Le pilotage automatique des essais triaxiaux, L'expérimentation en Génie Civil, AUGC Rencontres scientifiques, Nantes, 1995, 5–10.
10) Henkel, D. J. (1956): The effect of overconsolidation on the behaviour of clays during shear, *Géotechnique*, **6**, 139–150.
11) Hicher. P. Y. (1985): Comportement mécanique des argiles saturées sur divers chemins de sollicitations monotones et cycliques application à une modélisation élastoplastique et viscoplastique, *Thèse de doctorat d'état és sciences physiques Paris6* (in French).
12) Ishihara, K. and Okada, S. (1978): Effects of stress history on cyclic behavior of sands, *Soils and Foundations*, **18** (4), 31–45.
13) Kirkpatrick, W. M. (1961): Discussion on soil properties and their measurement, *Proc. 5th ICSMFE*, Paris, 131–133.
14) Lade, P. V. and Tsai, J. (1985): Effects of localization in triaxial tests on clays, *Proc. list ICSMFE*, San Franscisco, 549–552.
15) Luong, M. P. (1978): Etat caractéristique du sol, *C.R.Ac.Sc. t.287 série B*, **305**, Paris.
16) Parry, R. H. G. (1960): Triaxial compression and extension tests on remoulded saturated clay, *Geotechnique*, **10**, 166–180.
17) Pender, M. J. (1978): A model for the behaviour of overconsolidated soil, *Géotechnique*, **28** (1), 1–25.
18) Reynolds, O. (1885): On the dilatancy of media composed of rigid particles in contact, with experimental illustration, *Philosophical Magazine*, Series 5, **20**, 469–481.
19) Roscoe, K. H, Schofield, A. N. and Wroth, C. P. (1958). On the yielding of soils, *Geotechnique*, **8** (1), 22–53.
20) Rowe, P. W. (1962): The stress dilatancy relation for static equilibrium of an assembly of particles in contact, *Proc. Royal Society*, **A269**, 500–527.
21) Schofield, A. N. and Wroth, C. P. (1968): *Critical State Soil Mechanics*, McGraw Hill, New York.
22) Shimizu, M. (1982): Effect of overconsolidation on dilatancy of a cohesive soil, *Soils and Foundations* **22** (4), 121–133.
23) Taylor, N. (1948): *Fundamentals of Soil Mechanics*, Wiley, New York.

24) Wahyudi, H. (1991): Etude des propriétés mécaniques des matériaux argileux en relation avec leur organisation à différentes échelles, *Thèse de doctorat Ecole Centrale Paris Chatenay-Malabry* (in French).

25) Zervoyannis, C. (1982): Etude synthétique des propriétés mécaniques des argiles saturées et des sables sur chemin œdométrique et triaxial de révolution, *Thése de doctorat Ecole Centrale Paris Chatenay-Malabry* (in French).